



## A numerical treatment of a reaction-diffusion model of spatial pattern in the embryo

**S. Toubaei**

Islamic Azad University, Ahvaz Branch, Ahvaz, Iran.  
E-mail: stoobaei@yahoo.com

**M. Garshasbi\***

School of Mathematics, Iran University of Science and Technology, Tehran, Iran.  
E-mail: m.garshasbi@iust.ac.ir

**M. Jalalvand**

Department of Mathematics, Shahid Chamran University of Ahvaz, Ahvaz, Iran.  
E-mail: m.jalalvand@scu.ac.ir

---

**Abstract** In this work the mathematical model of a spatial pattern in chemical and biological systems is investigated numerically. The proposed model considered as a nonlinear reaction-diffusion equation. A computational approach based on finite difference and RBF-collocation methods is conducted to solve the equation with respect to the appropriate initial and boundary conditions. The ability and robustness of the numerical approach is investigated using two test problems.

---

**Keywords.** Reaction-Diffusion, ecological systems, RBF collocation.

**2010 Mathematics Subject Classification.** 65L05, 34K06, 34K28.

### 1. INTRODUCTION

Generally in science phenomenon is used to discuss any sign or objective symptom; any observable occurrence or fact. Recently geo-referenced objects and phenomena changing over time enjoy a lot of attention. Cadastral information systems with the need to record history of land parcels existence and ownership, navigational systems computing possible routes of vehicles in time, and environmental applications dealing with forecast prediction, especially in "sensitive" areas with typhoon and cyclone problems, are some substantial examples of this new application area [14, 17]. Identifying the complex relationships between ecological patterns and processes is a crucial task. One of the central issues in developmental biology is the understanding of the emergence of structure and form from the almost uniform mass of dividing cells that constitutes the early embryo. Although genes play a key role, genetics says nothing about the actual mechanisms which bring together the constituent parts into a coherent pattern [11, 15, 14]

Qualitatively and quantitatively, mathematical models play a vital role in analyzing ecological systems. In [15] the author demonstrated, theoretically, that a system of

---

Received: 2 August 2016 ; Accepted: 14 November 2016.

\* Corresponding author.

reacting and diffusing chemicals could spontaneously evolve to spatially heterogeneous patterns from an initially uniform state in response to infinitesimal perturbations. In this study it is shown that diffusion could drive a chemical system to instability, leading to spatial pattern where no prior pattern existed. The author considered a system of two chemicals, in which one was an activator and the other an inhibitor. He showed that if the diffusion of the inhibitor was greater than that of the activator, then diffusion-driven instability could result [11, 15].

Today the reaction-diffusion equations are widely used as models for spatial effects in ecology. They support three important types of ecological phenomena. These models emphasize that simple organism movement can produce striking largescale patterns in homogeneous environments and that in heterogeneous environments, movement of multiple species can change the outcome of competition or predation [2]. Reaction-diffusion invasion models exhibit more striking behavior when population growth is not exponential but instead is regulated by density-dependent mortality. These models produce travelling waves of invaders that spread out from their "beachhead" at a constant velocity and shape.

Usually finding the exact solution of reaction-diffusion equations specially the nonlinear equations is a complex task and in a lot of nonlinear PDE problems, one can not solve them analytically. In recent years considerable studies has been done in the numerical solution of nonlinear PDEs. The investigation of exact and numerical solutions for nonlinear partial differential equations (NLPDEs) plays an important role in the study of nonlinear physical phenomena. These solutions when they exist can help one to well understand the mechanism of the complicated physical phenomena and dynamical processes modelled by these nonlinear evolution equations.

In this paper the radial basis functions (RBF) collocation method and finite difference approach are used to solve a system of nonlinear reaction-diffusion model arises from the chemical systems.

Meshless methods based on the collocation method have been dominant and efficient. Considerable studies can be found regards to the application of RBF functions for solving PDE problems in literature [3, 4, 6, 7, 8, 10, 9, 18]. Numerical studies illustrates the advantages of using this mesh-less methods to solve initial and/or boundary value problems [9, 10]. The large number of recent research works on mesh-less methods especially RBF collocation method for solving nonlinear PDE's demonstrates the popularity that the methods have recently enjoyed.

This paper is organized as follows:

In section 2, the mathematical formulation of a spatial pattern in chemical and biological systems is presented. In section 3, a general form of the model introduced in section 2 is considered with appropriate initial and boundary conditions and a numerical procedure based on finite difference and RBF methods is established to solve this problem. Section 4 contains some test problems.

## 2. REACTION-DIFFUSION MODELLING

In this section we review the mathematical formulation of a spatial pattern in chemical and biological systems. Suppose that we have the simple autocatalytic process  $E + F \rightarrow 2F$  in an unstirred reactor initially full of chemical  $E$  but with



no chemical  $F$ . Therefore, there will be no reaction. Now if one seeds the reaction domain with some  $F$  at various local sites and if  $E$  can diffuse but  $F$  be immobilized, reaction will only occur where there has been seeding, with high concentrations of  $F$  building up at these points. Eventually,  $E$  would disappear and we would be left with "spots" of  $F$ . However, with this assumption that there is a supply of  $E$  across the domain and also a decay step for  $F$  to limit its growth, it is possible to get a balance between supply and diffusion away of  $E$  balancing the decay of  $F$  in the spots, to give steady-state, long-lived pattern, with high  $E$  concentrations in between the spots and high  $F$  concentration in the spots [11]. For mathematical modelling of these systems, generally the following reaction-diffusion equation is obtained [11, 14]

$$\frac{\partial u}{\partial t} = D \frac{\partial^2 u}{\partial x^2} + F(x, t, u, c), \quad (2.1)$$

where  $u$  is a vector representing chemical concentrations,  $D$  denotes the matrix of diffusion coefficients (assumed constant), and the second term represents chemical reactions, with kinetic parameters  $c$ , such as rate constants, production and degradation terms. The form of the  $F = (f, g)$  have been made and studied for many specific forms [5, 11, 12, 16].

Here we focus on a two-chemical system, in which  $u = (u_1, u_2)$  denotes the chemical concentrations and  $F = (f, g)$  has the specific forms of the kinetics  $f$  and  $g$  [11, 12, 16]. As reported in [11], when a sequence of reactions are occurred as follows



according to the law of mass action, the production of  $X$  may occur at the rate

$$k_1 a - k_1 u + k_3 u_1^2 u_2. \quad (2.3)$$

Furthermore the production of  $Y$  can occur at the rate

$$k_4 b - k_3 u_1^2 u_2, \quad (2.4)$$

where  $u_1$ ,  $u_2$ ,  $a$  and  $b$  are the concentrations of  $X, Y, E$  and  $F$ , respectively, and  $k_1, \dots, k_4$  are rate constants. Now if one assumes that  $X$  and  $Y$  diffuse with diffusion coefficients  $D_1$  and  $D_2$  respectively, and that  $E$  and  $F$  are in abundance so that  $a$  and  $b$  can be assumed approximately constant, the reaction diffusion system satisfied by  $u_1$  and  $u_2$  may be written as

$$\begin{cases} \frac{\partial u_1}{\partial t} = D_1 \frac{\partial^2 u_1}{\partial x^2} + k_1 a - k_1 u + k_3 u_1^2 u_2 \\ \frac{\partial u_2}{\partial t} = D_2 \frac{\partial^2 u_2}{\partial x^2} + k_4 b - k_3 u_1^2 u_2 \end{cases}. \quad (2.5)$$

Boundary conditions are usually taken as zero flux, that is, the domain boundary is assumed impermeable to the chemicals, but in this study we consider the proposed problem in general form with appropriate initial and boundary conditions. A numerical procedure based on RBF collocation and finite difference approaches is established to solve equation (2.5).



### 3. NUMERICAL SOLUTION

Consider the equation (2.5) in more general form to be solved over in domain  $\Omega = [0, 1] \times [0, 1]$  with enclosing initial and boundary conditions

$$\frac{\partial u_1}{\partial t} = D_1 \frac{\partial^2 u_1}{\partial x^2} - k_1 u + k_3 u_1^2 u_2 + F(x, t), \quad (x, t) \in \Omega, \quad (3.1)$$

$$\frac{\partial u_2}{\partial t} = D_2 \frac{\partial^2 u_2}{\partial x^2} - k_3 u_1^2 u_2 + G(x, t), \quad (x, t) \in \Omega, \quad (3.2)$$

$$u_1(x, 0) = f(x), \quad (3.3)$$

$$u_2(x, 0) = g(x), \quad (3.4)$$

$$\frac{\partial u_1}{\partial x}(0, t) = \varphi_1(t), \quad (3.5)$$

$$\frac{\partial u_1}{\partial x}(1, t) = \psi_1(t), \quad (3.6)$$

$$\frac{\partial u_2}{\partial x}(0, t) = \varphi_2(t), \quad (3.7)$$

$$\frac{\partial u_2}{\partial x}(1, t) = \psi_2(t), \quad (3.8)$$

It is considered that all functions in this problem are  $L_2$  known functions. To establish our proposed numerical procedure first we discretize the equations (3.1) and (3.2) by using the forward difference rule for time derivatives and the well known Crank-Nicolson scheme for other terms between successive time levels  $n$  and  $n + 1$ . Suppose  $\Delta t$  denotes the time step size,  $t_n = t_0 + n\Delta t$ ,  $U_1^n = u_1(x, t_n)$ ,  $U_2^n = u_2(x, t_n)$ ,  $F(x, t_n) = F^n$  and  $G(x, t_n) = G^n$ . Discretizing these equations obtains

$$\begin{aligned} \frac{U_1^{n+1} - U_1^n}{\Delta t} &= D_1 \frac{U_{1xx}^{n+1} + U_{1xx}^n}{2} - k_1 \frac{U_1^{n+1} + U_1^n}{2} \\ &\quad + k_3 \frac{(U_1^2)^{n+1} U_2^{n+1} + (U_1^2)^n U_2^n}{2} + F^n, \end{aligned} \quad (3.9)$$

$$\begin{aligned} \frac{U_2^{n+1} - U_2^n}{\Delta t} &= D_2 \frac{U_{2xx}^{n+1} + U_{2xx}^n}{2} - k_3 \frac{(U_1^2)^{n+1} U_2^{n+1} + (U_1^2)^n U_2^n}{2} \\ &\quad + G^n. \end{aligned} \quad (3.10)$$

By linearizing the nonlinear terms using the following formula which readily obtained by applying the Taylor expansion [13]

$$(UV)^{n+1} = U^{n+1}V^n + U^nV^{n+1} - U^nV^n. \quad (3.11)$$

The equations (3.9) and (3.10) may reform as

$$\begin{aligned} &2U_1^{n+1} - D_1\Delta tU_{1xx}^{n+1} + k_1\Delta tU_1^{n+1} - k_3\Delta t(2U_1^nU_2^nU_1^{n+1} + (U_1^n)^2U_2^{n+1}) \\ &= 2U_1^n + D_1\Delta tU_{1xx}^n - k_1\Delta tU_1^n - k_3\Delta t(U_1^n)^2U_2^n + F^n, \end{aligned} \quad (3.12)$$

$$\begin{aligned} &2U_2^{n+1} - D_2\Delta tU_{2xx}^{n+1} + k_3\Delta t(2U_1^nU_2^nU_1^{n+1} + (U_1^n)^2U_2^{n+1}) \\ &= 2U_2^n + D_2\Delta tU_{2xx}^n + k_3\Delta t(U_1^n)^2U_2^n + G^n. \end{aligned} \quad (3.13)$$



**3.1. The RBF collocation approach.** In this section, a computational procedure based on the collocation and RBF expansion methods is established to solve the problem (3.12)-(3.13) with respect to the initial and boundary conditions (3.3)-(3.8).

At collocation points  $x_i, i = 0, 1, \dots, N$  over  $[0, 1]$  such that  $x_i, i = 1, \dots, N - 1$  are interior points and  $x_i, i = 0, N$  are boundary points, we apply the following approximation

$$u_1(x, t_n) = U_1^n \simeq \sum_{j=0}^N \lambda_j^n \phi(r_j), \quad u_2(x, t_n) = U_2^n \simeq \sum_{j=0}^N \gamma_j^n \phi(r_j), \quad (3.14)$$

where  $n$  is the number of time iterations,  $N$  is the number of the data points,  $\lambda_j^n$  and  $\gamma_j^n, j = 0, 1, \dots, N$ , are the unknown coefficients to be determined later,  $r_j = |x - x_j|$  is the Euclidean norm between the points  $x$  and  $x_j$ . The function  $\phi(r)$  can be used as different RBFs such as  $\phi(r) = \sqrt{r^2 + \varepsilon^2}$  (MQ) or  $\phi(r) = \frac{1}{\sqrt{r^2 + \varepsilon^2}}$  (IMQ). In sequence our computations are conducted based on MQ functions.

The coefficients  $\lambda_j^n$  and  $\gamma_j^n, j = 0, 1, \dots, N$  in equation (3.14) can be determined using collocation approach. To this end for each time iteration  $n = 1, 2, \dots$ , the  $2N + 2$  unknown coefficients need to be determined from the boundary conditions given at  $x_0$  and  $x_N$  and collocating  $U_1^n$  and  $U_2^n$  at the remaining  $N - 1$  distinct uniformly distributed interior points  $x_i$  in  $[x_1, x_{N-1}]$  as

$$u_1(x_i, t_n) = U_{1i}^n \simeq \sum_{j=0}^N \lambda_j^n \phi(r_{ij}), \quad u_2(x_i, t_n) = U_{2i}^n \simeq \sum_{j=0}^N \gamma_j^n \phi(r_{ij}), \quad (3.15)$$

where  $r_{ij} = |x_i - x_j|$ . Computing the first and second derivatives of the approximate solutions and substituting the equations (3.15) into equations (3.12) and (3.13) at the collocation points  $x_i$  and using the boundary conditions one may obtain the following linear equations

$$\begin{aligned} & \left\{ 2 + k_1 \Delta t - 2k_3 \Delta t \left( \sum_{j=0}^N \lambda_j^n \phi(r_{ij}) \right) \left( \sum_{j=0}^N \gamma_j^n \phi(r_{ij}) \right) \right\} \left\{ \sum_{j=0}^N \lambda_j^{n+1} \phi(r_{ij}) \right\} \\ & - D_1 \Delta t \sum_{j=0}^N \lambda_j^{n+1} \phi''(r_{ij}) - k_3 \Delta t \left( \sum_{j=0}^N \lambda_j^n \phi(r_{ij}) \right)^2 \left( \sum_{j=0}^N \gamma_j^{n+1} \phi(r_{ij}) \right) \\ & = F_i^n + (2 - k_1 \Delta t) \sum_{j=0}^N \lambda_j^n \phi(r_{ij}) + D_1 \Delta t \sum_{j=0}^N \lambda_j^n \phi''(r_{ij}) \\ & - k_3 \left( \sum_{j=0}^N \lambda_j^n \phi(r_{ij}) \right)^2 \left( \sum_{j=0}^N \gamma_j^n \phi(r_{ij}) \right), \quad i = 1, \dots, N - 1, \end{aligned} \quad (3.16)$$



$$\begin{aligned}
 & \{2 + k_3 \Delta t (\sum_{j=0}^N \lambda_j^n \phi(r_{ij}))^2\} \{ \sum_{j=0}^N \gamma_j^{n+1} \phi(r_{ij}) \} - D_2 \Delta t \sum_{j=0}^N \gamma_j^{n+1} \phi''(r_{ij}) \\
 & + 2k_3 \Delta t (\sum_{j=0}^N \lambda_j^n \phi(r_{ij})) (\sum_{j=0}^N \gamma_j^n \phi(r_{ij})) (\sum_{j=0}^N \lambda_j^{n+1} \phi(r_{ij})) \\
 & = G_i^n + (2 + k_3 \Delta t (\sum_{j=0}^N \lambda_j^n \phi(r_{ij}))^2) (\sum_{j=0}^N \gamma_j^n \phi(r_{ij})) \\
 & + D_2 \Delta t \sum_{j=0}^N \gamma_j^n \phi''(r_{ij}), \quad i = 1, \dots, N - 1.
 \end{aligned} \tag{3.17}$$

Furthermore according to the boundary conditions one may write

$$\sum_{j=0}^N \lambda_j^{n+1} \phi'(r_{0j}) = \varphi_1(t_{n+1}), \tag{3.18}$$

$$\sum_{j=0}^N \lambda_j^{n+1} \phi'(r_{Nj}) = \psi_1(t_{n+1}), \tag{3.19}$$

$$\sum_{j=0}^N \gamma_j^{n+1} \phi'(r_{0j}) = \varphi_2(t_{n+1}), \tag{3.20}$$

$$\sum_{j=0}^N \gamma_j^{n+1} \phi'(r_{Nj}) = \psi_2(t_{n+1}). \tag{3.21}$$

Equations (3.16)-(3.21) determine a system of  $(2N+2)(2N+2)$  linear equations which can be written as

$$AX^{n+1} = b, \tag{3.22}$$

where

$$X^{n+1} = [\lambda_0^{n+1}, \lambda_1^{n+1}, \dots, \lambda_N^{n+1}, \gamma_0^{n+1}, \gamma_1^{n+1}, \dots, \gamma_N^{n+1}], \tag{3.23}$$

and the elements of the coefficient matrix  $A$  and the right hand side vector  $b$  can be easily read from the equations (3.16)-(3.21). Here the singular value decomposition (SVD) approach is used to solve the equation (3.22).

#### 4. NUMERICAL EXPERIMENTS

In this section, we implement the proposed method to solve the model equations presented in Section 2 based on MQ functions.

To investigate the ability and effectiveness of the proposed method, two numerical examples are considered. The discrete  $L_2$  and  $L_\infty$  error norms by using differences between the analytical and numerical results at the node points have been computed to verify the accuracy of the numerical results. For test problems whose analytical



solution is known, the following error norms will be used to measure the error between the analytical and numerical solutions

$$L_2 = \sqrt{h \sum_{j=0}^N |U_{exact}^j - U_{appr}^j|^2}, \quad (4.1)$$

$$L_\infty = \max_j |U_{exact}^j - U_{appr}^j|, \quad (4.2)$$

at the data points  $x_j$  where  $h = \frac{1}{N}$ . In the concept of RBFs it had been shown that the accuracy of the RBFs solution, depends heavily on the choice of the shape parameter  $\varepsilon$  spatially in the MQ or inverse IMQ basis functions. Recently some authors have focused on determination of optimal values for the shape parameters in RBFs for some special problems [3, 4]. Determination of suitable shape parameter is extracted experimentally for the RBFs used in this study. In our experiments the optimal value of  $\varepsilon$  is to be found numerically for each radial basis function and for each problem separately.

**Example 1.** In the problem (3.1)-(3.8) let

$$\begin{aligned} D_1 = 1, D_2 = 1, k_1 = 1, k_3 = 1, \\ f(x) = 2 + \frac{1}{1 + e^x}, \varphi_1(t) = -\frac{e^{3t}}{(1 + e^{3t})^2}, \psi_1(t) = -\frac{e^{1+3t}}{(1 + e^{1+3t})^2}, \\ g(x) = \frac{x}{1 + e^x}, \varphi_2(t) = \frac{1 - e^{3t}(-1 + t)}{(1 + e^{3t})^2}, \psi_2(t) = \frac{1 - e^{1+3t}t}{(1 + e^{1+3t})^2}. \end{aligned}$$

With these assumptions the exact solutions are considered as

$$u_1(x, t) = 2 + \frac{1}{1 + e^{3t+x}}, \quad u_2(x, t) = \frac{t + x}{1 + e^{3t+x}}.$$

The functions  $F(x, t)$  and  $G(x, t)$  can be extracted form the exact solutions.

This numerical example is studied by using mesh size  $h = 0.05$  and the time step  $\Delta t = 0.01$ .

Tables 1 and 2 respectively report the  $L_2$  and  $L_\infty$  error norms between the exact and approximate  $u_1$  and  $u_2$  at some time levels and for some shape parameters.

Throughout the simulation, the  $L_\infty$  and  $L_2$  error norms decrease with the smaller time step size. Nevertheless increasing time levels, degrease the accuracy of the solutions. The behavior of  $L_2$ -error norm at  $t = 0.5$  for computing  $u_1$  and  $u_2$  are shown in Figures 1 and 2.



TABLE 1. The values of  $L_\infty$  and  $L_2$  error norms versus the shape parameter in Example 1 at some times for  $u_1$ .

| Time | RBF | shape parameter $\varepsilon$ | $L_\infty$ error norm   | $L_2$ error norm        |
|------|-----|-------------------------------|-------------------------|-------------------------|
| 0.3  | MQ  | 0.25                          | $2.0976 \times 10^{-2}$ | $3.9831 \times 10^{-2}$ |
|      |     | 0.45                          | $4.0554 \times 10^{-3}$ | $5.6789 \times 10^{-3}$ |
|      |     | 0.65                          | $3.4831 \times 10^{-4}$ | $4.8876 \times 10^{-4}$ |
|      |     | 0.95                          | $1.6641 \times 10^{-2}$ | $3.0643 \times 10^{-2}$ |
| 0.5  | MQ  | 0.25                          | $4.6973 \times 10^{-2}$ | $5.3856 \times 10^{-2}$ |
|      |     | 0.45                          | $8.6754 \times 10^{-3}$ | $9.9759 \times 10^{-3}$ |
|      |     | 0.65                          | $7.8841 \times 10^{-4}$ | $8.8996 \times 10^{-4}$ |
|      |     | 0.95                          | $3.9641 \times 10^{-2}$ | $4.4843 \times 10^{-3}$ |
| 0.7  | MQ  | 0.25                          | $7.0976 \times 10^{-2}$ | $8.8831 \times 10^{-2}$ |
|      |     | 0.45                          | $9.0754 \times 10^{-2}$ | $9.9779 \times 10^{-2}$ |
|      |     | 0.65                          | $3.2841 \times 10^{-3}$ | $4.8906 \times 10^{-3}$ |
|      |     | 0.95                          | $8.9641 \times 10^{-2}$ | $9.0643 \times 10^{-2}$ |

TABLE 2. The values of  $L_\infty$  and  $L_2$  error norms versus the shape parameter in Example 1 at some times for  $u_2$ .

| Time | RBF | shape parameter $\varepsilon$ | $L_\infty$ error norm   | $L_2$ error norm        |
|------|-----|-------------------------------|-------------------------|-------------------------|
| 0.3  | MQ  | 0.25                          | $3.1236 \times 10^{-2}$ | $3.9941 \times 10^{-2}$ |
|      |     | 0.45                          | $2.3554 \times 10^{-3}$ | $3.5789 \times 10^{-3}$ |
|      |     | 0.65                          | $1.4431 \times 10^{-4}$ | $2.8326 \times 10^{-4}$ |
|      |     | 0.95                          | $4.3641 \times 10^{-3}$ | $9.6743 \times 10^{-3}$ |
| 0.5  | MQ  | 0.25                          | $4.7893 \times 10^{-2}$ | $5.2836 \times 10^{-2}$ |
|      |     | 0.45                          | $6.6754 \times 10^{-3}$ | $7.9756 \times 10^{-3}$ |
|      |     | 0.65                          | $5.8741 \times 10^{-4}$ | $6.8456 \times 10^{-4}$ |
|      |     | 0.95                          | $2.3641 \times 10^{-2}$ | $3.2843 \times 10^{-2}$ |
| 0.7  | MQ  | 0.25                          | $8.3976 \times 10^{-2}$ | $8.9733 \times 10^{-2}$ |
|      |     | 0.45                          | $2.0754 \times 10^{-2}$ | $3.3779 \times 10^{-2}$ |
|      |     | 0.65                          | $4.2231 \times 10^{-3}$ | $5.1896 \times 10^{-3}$ |
|      |     | 0.95                          | $9.6941 \times 10^{-2}$ | $9.9943 \times 10^{-2}$ |

**Example 2.** In the problem (3.1)-(3.8) let

$$\begin{aligned}
 D_1 &= 4, \quad D_v = 1, \quad k_1 = 2, \quad k_3 = 2, \\
 F(x, t) &= 4 \sinh(3t + x) \tanh^2(3t + x) + \operatorname{sech}^2(3t + x) (3 + 8 \tanh^3(3t + x)), \\
 G(x, t) &= 6 \cosh(3t + x) - 2(1 + 3 \cosh(3t + x)) \tanh^3(3t + x) \\
 &\quad + \operatorname{sech}^2(3t + x) (3 + 2 \tanh^3(3t + x)), \\
 f(x) &= \tanh(x), \quad \varphi_1(t) = \operatorname{sech}^2(3t), \quad \psi_1(t) = \operatorname{sech}^2(1 + 3t), \\
 g(x) &= 2 \sinh(x) + \tanh(x), \quad \varphi_2(t) = 2 \cosh(3t) + \operatorname{sech}^2(3t), \\
 \psi_2(t) &= 2 \cosh(1 + 3t) + \operatorname{sech}^2(1 + 3t).
 \end{aligned}$$





FIGURE 1. The  $L_2$ -error norm between the exact and approximate solutions for  $u_1(x, t)$  with respect to the shape parameter  $\varepsilon$  at  $t = 0.5$  for Example 1.

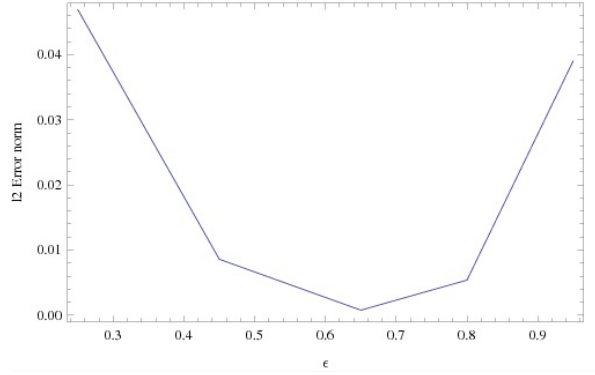
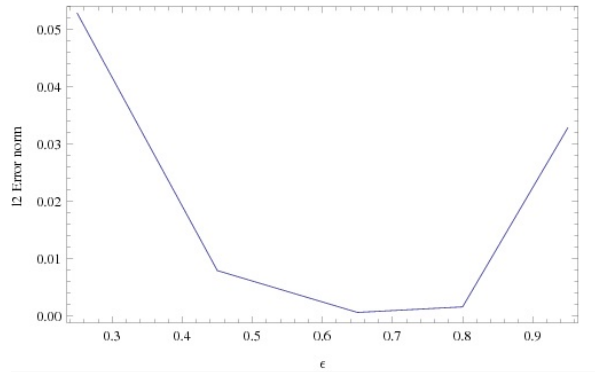


FIGURE 2. The  $L_2$ -error norm between the exact and approximate solutions for  $u_2(x, t)$  with respect to the shape parameter  $\varepsilon$  at  $t = 0.5$  for Example 1.



With these assumptions the exact solutions can be obtained as

$$u_1(x, t) = \tanh(3t + x), \quad u_2(x, t) = 2 \sinh(3t + x) + \tanh(3t + x).$$

This numerical example is studied by using mesh size  $h = 0.05$  and the time step  $\Delta t = 0.01$ .

Tables 3 and 4 respectively demonstrate the  $L_\infty$  and  $L_2$  error norms between the exact and approximate  $u_1$  and  $u_2$  at some time levels and for some shape parameters.

For this problem, similar to the the previous problem, different shape parameters are investigated via our computation. Throughout the simulation it was seen that the  $L_\infty$  and  $L_2$  error norms decrease with the smaller time step size. In addition increasing



TABLE 3. The values of  $L_\infty$  and  $L_2$  error norms versus the shape parameter in Example 2 at some times for  $u_1$ .

| Time | RBF | shape parameter $\varepsilon$ | $L_\infty$ error norm   | $L_2$ error norm        |
|------|-----|-------------------------------|-------------------------|-------------------------|
| 0.3  | MQ  | 0.15                          | $1.3462 \times 10^{-3}$ | $1.9833 \times 10^{-3}$ |
|      |     | 0.35                          | $7.3454 \times 10^{-3}$ | $9.8989 \times 10^{-3}$ |
|      |     | 0.55                          | $5.3431 \times 10^{-2}$ | $5.0876 \times 10^{-2}$ |
|      |     | 0.75                          | $8.5641 \times 10^{-2}$ | $9.9643 \times 10^{-2}$ |
| 0.5  | MQ  | 0.15                          | $3.3173 \times 10^{-3}$ | $3.8836 \times 10^{-3}$ |
|      |     | 0.35                          | $8.8854 \times 10^{-3}$ | $9.9959 \times 10^{-3}$ |
|      |     | 0.55                          | $7.3441 \times 10^{-2}$ | $8.0996 \times 10^{-2}$ |
|      |     | 0.75                          | $9.0964 \times 10^{-2}$ | $9.9893 \times 10^{-2}$ |
| 0.7  | MQ  | 0.15                          | $7.4576 \times 10^{-3}$ | $8.8981 \times 10^{-3}$ |
|      |     | 0.35                          | $2.0754 \times 10^{-2}$ | $3.1977 \times 10^{-2}$ |
|      |     | 0.55                          | $8.0841 \times 10^{-2}$ | $9.1890 \times 10^{-2}$ |
|      |     | 0.75                          | $4.9741 \times 10^{-1}$ | $5.1645 \times 10^{-1}$ |

TABLE 4. The values of  $L_\infty$  and  $L_2$  error norms versus the shape parameter in Example 2 at some times for  $u_2$ .

| Time | RBF | shape parameter $\varepsilon$ | $L_\infty$ error norm   | $L_2$ error norm        |
|------|-----|-------------------------------|-------------------------|-------------------------|
| 0.3  | MQ  | 0.15                          | $2.3236 \times 10^{-3}$ | $2.9341 \times 10^{-3}$ |
|      |     | 0.35                          | $2.9854 \times 10^{-3}$ | $3.1789 \times 10^{-3}$ |
|      |     | 0.55                          | $3.8431 \times 10^{-2}$ | $3.9832 \times 10^{-2}$ |
|      |     | 0.75                          | $4.7643 \times 10^{-2}$ | $5.6735 \times 10^{-2}$ |
| 0.5  | MQ  | 0.15                          | $3.0786 \times 10^{-3}$ | $3.2846 \times 10^{-3}$ |
|      |     | 0.35                          | $4.2754 \times 10^{-3}$ | $4.8956 \times 10^{-3}$ |
|      |     | 0.55                          | $5.3471 \times 10^{-2}$ | $5.8846 \times 10^{-2}$ |
|      |     | 0.75                          | $7.0341 \times 10^{-2}$ | $7.2943 \times 10^{-2}$ |
| 0.7  | MQ  | 0.15                          | $6.0376 \times 10^{-3}$ | $6.6738 \times 10^{-3}$ |
|      |     | 0.35                          | $7.0734 \times 10^{-2}$ | $7.3459 \times 10^{-2}$ |
|      |     | 0.55                          | $9.4331 \times 10^{-2}$ | $9.8896 \times 10^{-2}$ |
|      |     | 0.75                          | $4.0946 \times 10^{-1}$ | $4.9967 \times 10^{-1}$ |

time levels, decrease the accuracy of the solutions. The behavior of  $L_2$ -error norm at  $t = 0.5$  for computing  $u_1$  and  $u_2$  are shown in Figures 3 and 4.

### 5. CONCLUSION

In this study a mathematical model of a spatial pattern in chemical and biological systems is considered as a nonlinear reaction-diffusion equation. A numerical approach based on RBF collocation and finite difference methods is established to solve the proposed model numerically. To this end an important type of RBFs namely MQ are used. The numerical results show a good agreement between the exact and numerical solutions.



FIGURE 3. The  $L_2$ -error norm between the exact and approximate solutions for  $u_1(x, t)$  with respect to the shape parameter  $\epsilon$  at  $t = 0.5$  for Example 2.

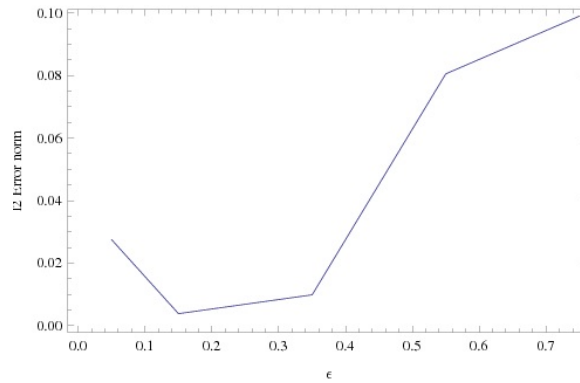
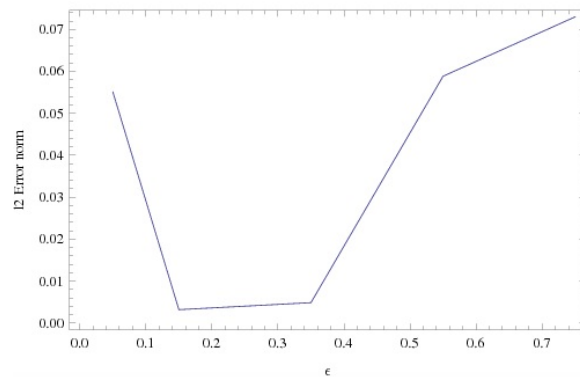


FIGURE 4. The  $L_2$ -error norm between the exact and approximate solutions for  $u_2(x, t)$  with respect to the shape parameter  $\epsilon$  at  $t = 0.5$  for Example 2.



## REFERENCES

- [1] R. S. Cantrell and C. Cosner, *Spatial Ecology via Reaction-Diffusion Equations*, Wiley, Chichester, 2003.
- [2] C. Cosner, *Reaction-Diffusion Equations and Ecological Modeling Tutorials in Mathematical Biosciences IV*, Lect. Not. Math., 1922 (2008), 77–115.
- [3] G. E. Fasshauer, J. G. Zhang, *On choosing optimal shape parameters for RBF approximation*, Numer. Algor., 45 (2007), 345–368. DOI 10.1017/CBO9780511791253.
- [4] B. Fornberg, C. Piret, *On choosing a radial basis function and a shape parameter when solving a convective PDE on a sphere*, J. Comput. Phys., 227 (2008), 2758–2780.
- [5] A. Gierer, H. Meinhardt, *A theory of biological pattern formation*, Kybernetik, 12 (1972), 30-39.



- [6] Y. C. Hon, R. Schaback, *On unsymmetric collocation by radial basis functions*, Appl. Math. Comput., 119 (2001), 177–186.
- [7] S. Hubbert, Closed form representations for a class of compactly supported radial basis functions, Adv. Comput. Math., 36 (2012), 115–136.
- [8] E. J. Kansa, Multiquadrics, *A scattered data approximation scheme with applications to computational fluid-dynamics, I Surface approximations and partial derivative estimates*, Comput. Math. Appl., 19 (1990), 127–145.
- [9] A. La Rocca, A. Hernandez Rosales and H. Power, *Radial basis function Hermite collocation approach for the solution of time dependent convectiondiffusion problems*, Engin. Anal. Bound. Elem., 29 (2005), 359–370.
- [10] J. Li, A. H. D. Cheng, C. S. Chen, *A comparisons of efficiency and error convergence of multiquadric collocation method and finite element method*, Eng. Anal. Bound. Elem., 27 (2003), 251–257.
- [11] P. K. Maini, K. J. Painter, H. N. P. Chauh, *Spatial pattern formation in chemical and biological systems*, J. Chem. Soc., Faraday Trans., 93 (1997), 3601–3610.
- [12] G. Nicolis, I. Prigogine, *Self-Organization in Non-Equilibrium Systems: From Dissipative Structures to Order Through Fluctuations*, Wiley, New York, 1977.
- [13] S. G. Rubin, R.A. Graves, *Cubic Spline Approximation for Problems in Fluid Mechanics* Nasa TR R-436, Washington, D.C., 1975.
- [14] N. Tryfona, *Modeling Phenomena in Spatiotemporal Databases: Desiderata and Solutions*, Lecture Notes in Computer Science, Springer-Verlag, 2006.
- [15] A. M. Turing, *Philosophical Transactions of the Royal Society of London. Series B, Biol. Sci.*, 237 (1952), 37–72.
- [16] M. J. Ward, *Asymptotic Methods for Reaction-Diffusion Systems: Past and Present*, Bull. Math. Bio., 68 (2006), 1151–1167.
- [17] M. Worboys, *A Unified Model for Spatial and Temporal Information.*, The Computer Journal, 37 (1994), 26–34.
- [18] J. Yoon. *Spectral approximation orders of radial basis function interpolation on the Sobolev space*. SIAM J. Math. Anal., 33 (2001), 946–958.

